A Rapid, Low-Cost Approach to Coastal Vulnerability Assessment at a National Level

Author(s): Mireia López Royo , Roshanka Ranasinghe , and José A. Jiménez
Source: Journal of Coastal Research, 32(4):932-945.
Published By: Coastal Education and Research Foundation
DOI: http://dx.doi.org/10.2112/JCOASTRES-D-14-00217.1
URL: http://www.bioone.org/doi/full/10.2112/JCOASTRES-D-14-00217.1

Journal of Coastal Research	32	4	932–945	Coconut Creek, Florida	July 2016

TECHNICAL COMMUNICATIONS

www.cerf-jcr.org

A Rapid, Low-Cost Approach to Coastal Vulnerability Assessment at a National Level

Mireia López Royo[†], Roshanka Ranasinghe[†‡§]*, and José A. Jiménez[††]

[†]Department of Water Science & Engineering
UNESCO-IHE Institute for Water Education
AX Delft 2611, The Netherlands

[‡]Research School of Earth Sciences
Australian National University
Canberra, ACT 0200, Australia

[§]Harbour, Coastal and Offshore Engineering
Deltares
MH Delft 2600, The Netherlands

[††]Laboratori d'Enginyeria Marítima
Universitat Politecnica de Catalunya-Barcelona Tech
Barcelona 08034, Spain

www.JCRonline.org

ABSTRACT

López Royo, M.; Ranasinghe, R., and Jiménez, J.A., 2016. A rapid, low-cost approach to coastal vulnerability assessment at a national level. *Journal of Coastal Research,* 32(4), 932–945. Coconut Creek (Florida), ISSN 0749-0208.

Vulnerability is defined as the system's potential to be damaged by a certain climate change (CC) hazard, and ideally, it has to be assessed by accounting for the different factors controlling the coastal response both in negative (susceptibility) and positive (resilience) terms to changing climatic and/or geomorphic conditions. The lack of an easy-to-use assessment method that requires only readily available data has severely hampered efforts to assess national-scale coastal vulnerability to the potential impacts of CC and population growth in the coastal zone, particularly when project budgets are limited. This study presents a modified version of the Coastal Vulnerability Index (CVI) approach. The main modifications are (1) the introduction of a more physically meaningful representation of the wave effect where storm erosion will only occur when the wave height exceeds a certain threshold value, and (2) an aggregated coastal-vulnerability classification method that comprises exactly the same number of vulnerability classes as that of the individual components of the CVI. As a demonstration, the method is applied to the 4996-km-long peninsular coastline of Spain. Under the worst-case scenario considered (sea-level rise [SLR] of 1 m by 2100), 50% of the Spanish coastline is classified as highly or very highly vulnerable. Given that tourism contributes 10% of the Spanish gross domestic product (GDP), it is noteworthy that high/very high vulnerability (both under low and high emissions scenarios) is indicated for very popular touristic areas along the Mediterranean Coast. These outcomes are likely to enable coastal managers/planners to identify high priority areas for further, more-detailed coastal vulnerability/hazard/risk quantification studies.

ADDITIONAL INDEX WORDS: *Climate change, sea-level rise, Spain, national scale assessment.*

INTRODUCTION

The projections given by the Intergovernmental Panel on Climate Change (IPCC, 2007) indicate a globally averaged sea level rise (SLR) of 0.18 m to 0.79 m (by 2090–2099 relative to 1980–1999), including an allowance of 0.2 m for uncertainty associated with ice sheet flow (*Note:* this study was completed before the release of the IPCC Fifth Assessment Report (AR5). Therefore, IPCC AR4 projections are used throughout this article). Future storms are expected to become more intense, with larger peak wind speeds and heavier precipitation. Average wave conditions (wave height and direction) are also expected to be modified by CC (Grabemann and Weisse, 2008; Hemer *et al.*, 2013). These CC-driven variations in environmental forcing are likely to result in significant physical impacts along coastlines around the world. For example, SLR will lead to coastal recession (Bruun, 1962; Ranasinghe, Callaghan, and Stive, 2012; Ranasinghe and Stive, 2009), whereas a slight shift in the average wave direction may lead to the realignment of embayed beaches (Slott *et al.*, 2006).

The potentially massive impact of CC on the world's coastal zones is now globally recognized (Gatriot *et al.*, 2008; Nicholls *et al.*, 2007; Ranasinghe *et al.*, 2013). Moreover, continued human attraction to the coast has resulted in rapid expansions in settlements, urbanization, infrastructure, economic activities, and tourism. The combination of coastal CC impacts and the ever-increasing human use of the coastal zone are very likely to result in unprecedented socioeconomic and environmental losses in the coming decades (Brown *et al.*, 2014). The potential losses along the highly developed and inhabited coastlines of northern Europe, northeastern America, southeastern Australia, and South Asia will be particularly high. To avoid such losses, it is imperative that risk-informed and sustainable

DOI: 10.2112/JCOASTRES-D-14-00217.1 received 28 October 2014; accepted in revision 23 March 2015; corrected proofs received 4 July 2015.

*Corresponding author: r.ranasinghe@unesco-ihe.org

coastal planning/management strategies are developed and implemented sooner rather than later. This requires comprehensive coastal risk assessments, which combine state-of-the-art consequence (or damage) modelling and coastal hazard modelling.

To limit the substantial amount of resources that need to be expended on a detailed coastal risk assessment, the first step is to undertake a coastal-vulnerability study. This enables the isolation of areas for which detailed risk assessments are required. Coastal vulnerability assessments may be undertaken at a variety of spatial scales: global, regional, national or subnational, and local. Well-known methods for determining coastal vulnerability spanning all of the above spatial scales include the Dynamic Interactive Vulnerability Assessment (DIVA) tool (Hinkel and Klein, 2009; Hinkel *et al*., 2013; Vafeidis *et al*., 2008), the Synthesis and Upscaling of Sea-level Rise Vulnerability Assessment Studies (SURVAS) (SURVAS, 2004), and the IPCC common methodology (CM) (IPCC CZMS, 1992). Vulnerability-assessment methods that are specifically suited for national- or subnational-scale applications include the *smartline approach* (Sharples *et al*., 2009) and the Coastal Vulnerability Index (CVI) (Gornitz and Kanciruk, 1989). Methods that have been developed to assess coastal vulnerability at local scale include the SimCLIM (CLIMsytems, 2007) and the Community Vulnerability Assessment Tool (CVAT) (NOAA Coastal Services Centre, 1999). For a detailed listing and summary descriptions of the above methods and their applications, the interested reader is referred to Abuodha (2009) and UNFCCC (2008).

The present study focuses on national-scale vulnerability assessment. All of the currently available methods/tools for national-level coastal vulnerability assessments require expert knowledge, expertise in using the tools, significant training in using the tools correctly, or all of the above. Therefore, especially for nations with strict budgetary constraints, the use of these existing methods/tools is suboptimal. This study was, therefore, undertaken with the specific aim of developing a rapid vulnerability assessment method that could be applied at a national scale with limited expert knowledge, expertise in using the tools, or training. The method developed herein, which is a modified version of the CVI method originally developed by Gornitz and Kanciruk (1989), is intended as a first-pass coastal-vulnerability assessment method, which could then be followed up with more detailed subnational/local scale vulnerability and/or risk assessments.

Here, coastal vulnerability is defined as the system's potential to be damaged by the combined effects of coastal inundation and erosion hazards. Thus, the vulnerability assessment needs to account for the different factors governing both negative (susceptibility) and positive (resilience) coastal response to changing climatic conditions. This method does not take into account social, economic, or cultural analyses of damage due to hazards, but focuses entirely on physical impacts of inundation and erosion. The two main attributes of the method are (1) it requires data that are easily accessible, and (2) it must be easy to use. As a demonstration case study, the method was applied to the 4996-km-long, peninsular coastline of Spain.

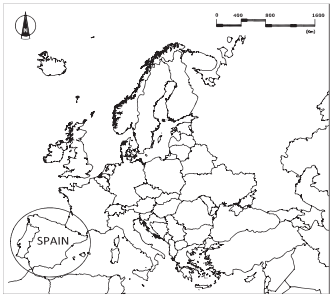

Figure 1. Study area.

Study Area

Figure 1 shows the Spanish coastline, which is 7880 km long, if the Canary Islands, the Balearic Islands, and Ceuta and Melilla are all taken into account. However, this study only focuses on the main, peninsular coast of Spain, which is 4996 km long (Ministerio de Agricultura, Alimentación y Medio Ambiente, 2002).

The Cantabrian and Galician Atlantic Coasts

This part of the coast experiences a temperate climate, in which squalls are quite frequent, and a high relative humidity. The mean tidal range along this coast is greater than 4 m, and waves are predominantly incident from NW. Mountain ranges that extend right up to the coast are common in this region. The coast experiences frequent high-energy storms and is frequently interrupted by tidal inlets. Ria-type lagoons and barrier estuaries are quite common along this coastline (Cendrero, Sánchez-Arcilla Conejo, and Zazo Cardeña, 2005).

The Atlantic Andalusian Coast

The southern Spanish Atlantic coast consists of a highly developed cliff/dune system and experiences large tides (2–3 m) and more-energetic SW waves. This coast is generally known as the Gulf of Cádiz and contains long, straight, sandy beaches backed by the aforementioned cliffs/dunes. Some barrier estuaries and lowlands are also present (Cendrero, Sánchez-Arcilla Conejo, and Zazo Cardeña, 2005).

The Mediterranean Coast

The Mediterranean Spanish coast contains more sandy beaches than the Spanish Atlantic coast does. In general, this long, extended stretch contains the longest uninterrupted beaches in Spain. The significant N-S longshore sediment transport along this coast, in conjunction with the rapid reduction of fluvial sediment supply from human activities has resulted in substantial erosion along this part of the Spanish coastline. The mean tidal range along this coast is less than 1 m, and waves are predominantly incident from the east. Several barrier estuaries with large ebb deltas, coastal wetlands, and some dune chains are also present.

The original version of the CVI has previously been applied twice in Spain, albeit at subnational scales, along the Catalonian coast (Martí López, 2011) and along the Andalusian coast (Ojeda Zújar *et al*., 2009). In addition to that, some specific aspects of coastal vulnerability and risk in Spain are reported

by Bosom and Jiménez (2011); Domínguez, Anfuso, and Gracia (2005); Málvarez García, Pollard, and Domínguez Rodríguez (2000); and Mendoza and Jiménez (2006). However, this is the first time, to our knowledge, that a national-scale coastal-vulnerability assessment has been undertaken in Spain.

METHODS

The method proposed in the present study is, in essence, a modified version of the CVI introduced by Gornitz and Kanciruk (1989). Although six different formulations of the CVI were initially proposed, CVI_5, which is the most commonly adopted version, will be used in this study:

$$CVI_5 = \sqrt{\frac{(x_1 x_2 x_3 x_4, \ \ldots, \ x_n)}{n}} \quad (1)$$

As can be seen from Equation (1), any number of parameters may be used in estimating the CVI. In this study, the same parameters adopted by the U.S. Geological Survey (USGS, 2004) in their national assessment of coastal vulnerability (Pendleton, Williams and Thieler, 2004; Pendleton *et al.*, 2004; Thieler and Hammar-Klose, 2000a,b), will be adopted. These parameters are x_1= geomorphology; x_2 = shoreline erosion/accretion; x_3 = coastal slope; x_4 = relative SLR; x_5 = wave height; and x_6 = tidal range.

Within the generally adopted CVI approach, each of the above parameters are then classified from 1 (very low vulnerability) to 5 (very high vulnerability). Subsequently, these parameter values are used in Equation (1) to calculate the composite CVI value for all the different coastal stretches that combine to form the national coastline. Based on the range of CVI values thus calculated, the vulnerability of each coastal stretch is classified as *low*, *medium*, *high*, or *very high*, depending on which percentile range (0–25, 25–50, 50–75, and 75–100%) a given stretch falls with the CVI. For a first-pass, national-scale study, relatively low-resolution information on the individual parameters is sufficient.

Components of the CVI

Each component of the CVI assesses a feature that has a certain influence to the overall vulnerability of the coast and is, therefore, quantified accordingly.

x_1: Geomorphology

This parameter expresses the relative erodibility of different landform types (*e.g.*, rocky cliffs, sandy beaches) along the coast and requires information on the spatial distribution of landform types and their stability. The type of geomorphologic data required for CVI applications is generally available in most countries. The spatial resolution at which this information is required will depend on the scale of the study area. In general, the more erodible the coastline is, the more vulnerable it is. For vulnerability assessments with time horizons of about a century (as is common in CC impact assessments), geomorphology may be considered as a temporally constant parameter because geomorphic variations in time generally occur at much-larger timescales than a century.

x_2: Shoreline Erosion/Accretion

The observed historical shoreline erosion/accretion trend is an indicator of the potential impact of CC and can be considered as a measure of the adaptation capacity of the coast. Thus, the vulnerability of historically accreting coasts (*i.e.* shoreline advances seaward) will be low. In contrast, eroding coasts (shoreline retreats landward) will be very sensitive to CC impacts, and thus, the vulnerability therein will be high. Historical shoreline-evolution information can be relatively easily gleaned from aerial photographs, satellite imagery, and if necessary, from Google Earth 7.0.2.8415beta (2015).

x_3: Coastal Slope

Following previous studies from Pendleton *et al.* (2004) and Thieler and Hammar-Klose (2000a,b), we consider the coastal slope to be a combination of both the subaerial beach profile and the submerged slope. This choice was made because the former is linked only to the inundation vulnerability, whereas the latter represents the potential for erosion, which is governed more by surfzone processes, such as wave breaking and undertow, and hence a direct function of the slope of the submerged profile (Komar, 1998). This approach will thus represent the vulnerability to the combined effect of inundation and erosion with milder slopes representing high vulnerability and steeper slopes representing low vulnerability. Subaerial slope can be obtained from generally available, national-topography databases or Google Earth 7.0.2.8415beta (2015), whereas submerged slopes may be obtained from the General Bathymetric Chart of the Oceans (GEBCO) (GEBCO, 2014) with an accuracy level sufficient for national-scale CVI applications.

x_4: Relative SLR

Relative sea-level change projections for a specific location generally account for the different contributions from various components at the global, regional, and local scales, as relevant to the study area (Nicholls *et al.*, 2014). These can be summed up for a given site using following equation:

$$\Delta RSL = \Delta SL_G + \Delta SL_{RM} + \Delta SL_{RG} + \Delta SL_{VLM} \quad (2)$$

where ΔRSL is the change in relative sea level; ΔSL_G is the change in global mean sea level; ΔSL_{RM} is the regional variation in sea level from the global mean due to meteo-oceanographic factors; ΔSL_{RG} is the regional variation in sea level due to changes in the earth's gravitational field; and ΔSL_{VLM} is the change in sea level due to vertical land movement.

At a national scale, relative SLR can be considered more or less spatially uniform, except for very long coastlines (*e.g.*, Australia, Canada, the United States), which may be subjected to different regional affects and along coastlines where spatially different vertical land-mass movements are present.

Because there is significant uncertainty associated with IPCC projected sea-level rise estimates, CVI applications generally account for the full range of IPCC-projected SLR estimates. The various SLR projections given by IPCC (2007) for different greenhouse gas emission scenarios (classified into three main classes) are shown in Table 1. If significant in the study area, the other contributors for relative SLR (RSLR; Equation 2) are added to/subtracted from the eustatic SLR values given in Table 1. To span the full range of IPCC projections, and as regional effects are generally smaller than the eustatic SLR, the method presented herein classifies the

potential vulnerability due to RSLR as low, moderate, high, and very high vulnerability for SLR projections (by 2100) of 0–0.18 m (low-emission scenario), 0.18–0.38 m (medium-emission scenario), 0.38–0.59 m (high-emission scenario), and 0.59–1 m (worst-case scenario).

x_5: Wave Climate

Previous CVI applications at a national scale (Abuodha and Woodroffe, 2006; Ojeda Zújar *et al.*, 2009; Pendleton *et al.*, 2004; Thieler and Hammar-Klose, 2000a,b) simply classified coastal vulnerability directly according to mean wave height (H) to represent the potential for storm erosion. A more scientifically defendable approach, which better represents potential storm erosion, is used in the method presented in this article. It is well known that storm erosion is directly related to the energy contained in storm waves and that the wave height has to be above a certain threshold (which depends on local conditions) to cause beach/dune erosion. Wave energy is proportional to H^2 and is given by the following equation

$$E = \frac{1}{8} \times \rho \times g \times H^2 \quad (3)$$

where E is wave energy, ρ is water density, g is the gravitational acceleration, and H is wave height.

In the present method, the storm erosion-nduced coastal vulnerability is represented by Equation (4):

$$\frac{H^2_{s_{95\%}}}{H^2_{s_{threshold}}} \quad (4)$$

where $H^2_{s_{95\%}}$ is the wave height that is exceeded only 5% of the time (or 95th percentile wave height) at each location where wave data are measured (or extracted from hindcasts) along the coast, and $H^2_{s_{threshold}}$ is the locally adopted threshold for storm definition. This threshold defines a storm at each location, and its value depends very much on the local conditions. The criterion is that a sufficient number of storms (preferably several dozen or more) can be identified in the long-term time record (to be considered a storm each individual event must occur at least 5 days before the next identified event). Although offshore wave data are becoming increasingly available around the world, in situations where no measured data are available, global hindcasts such as ERA-40 (European Centre for Medium-Range Weather Forecasts) or WW3 (Wavewatch III, National Oceanic and Atmospheric Administration) may also be used to quantify the parameter given in Equation (4). A value of 1 for the above parameter represents high vulnerability, whereas a value around 0.5 represents a very low vulnerability.

x_6: Tidal Range

The tidal range represents coastal vulnerability to flooding, both permanent and episodic. In their CVI application for the United States, Pendleton *et al.*, (2004) classified microtidal coasts to be of high vulnerability and macrotidal coasts to be of low vulnerability. This classification is justified by the following argumentation. At microtidal coasts, the sea level is always quite close to high tide; therefore, in the event of a storm surge, flooding is more likely than at macrotidal coasts. At macrotidal coasts, on the other hand, it is not unlikely that the sea level during a storm surge event is significantly lower than the high-tide level, thus increasing the possibility of reduced flood risk (Rosen, 1977). Although noting that there is some debate concerning this rationale (Kokot, Codignotto, and Elissondo, 2004), this approach is nevertheless adopted in the method used in this study. Tidal information is generally widely available around the world *via* direct measurements and/or global tide models, such as MIKE by DHI.

Table 1. *Classification of the Greenhouse gas emission scenarios from IPCC projections into three categories.*

		Sea-Level Rise Projections by 2100	
Category	Scenarios	m	mm/y
Low emission	B1[a]	0.18–0.38	1.5–3.9
	B2[b]	0.2–0.43	2.1–5.6
Medium emission	A1B[c]	0.21–0.48	2.1–6
	A1T[c]	0.2–0.45	1.7–4.7
High emission	A2[d]	0.23–0.51	3.0-8.5
	A1FI[c]	0.26–0.59	3.0–9.7

[a] B1 = A scenario family which describes a convergent world with the same global population that peaks in midcentury and declines thereafter, but with rapid changes in economic structures toward a service and information economy, with reductions in material intensity, and the introduction of clean and resource-efficient technologies. The emphasis is on global solutions to economic, social, and environmental sustainability, including improved equity, but without additional climate initiatives.

[b] B2 = A scenario family which describes a world in which the emphasis is on local solutions to economic, social, and environmental sustainability. It is a world with continuously increasing global population at a rate lower than A2, intermediate levels of economic development, and less rapid and more diverse technological change than in the B1 and A1 storylines. While the scenario is also oriented toward environmental protection and social equity, it focuses on local and regional levels.

[c] A1 = A scenario family that describes a future world of very rapid economic growth, global population that peaks in mid-century and declines thereafter, and the rapid introduction of new and more efficient technologies. Major underlying themes are convergence among regions, capacity building, and increased cultural and social interactions, with a substantial reduction in regional differences in per capita income. The A1 scenario family develops into three groups that describe alternative directions of technological change in the energy system: fossil intensive (A1FI), non-fossil energy sources (A1T), and balance across all sources (A1B).

[d] A2 = A scenario family which describes a very heterogeneous world. The underlying theme is self-reliance and preservation of local identities. Fertility patterns across regions converge very slowly, which results in continuously increasing global population. Economic development is primarily regionally oriented and per capita economic growth and technological change are more fragmented and slower than in other storylines.

Apart from the parameter *Geomorphology*, which can safely be assumed to be temporally invariable at planning timescales (generally <100 y), all other parameters may vary in time, especially because of CC effects. However, given that there is only sufficient information on how SLR might evolve in the future, as has been done in most previous vulnerability studies, all parameters other than SLR are taken to be temporally invariable (*i.e.* stationary) herein.

Aggregation Procedure

To apply the CVI at a national scale, first the coastline needs to be discretized into a number of stretches (*cells*), each of which can only have one vulnerability class for each parameter that is considered in Equation (1). The number of stretches will, therefore, be determined by the spatial variation of the six

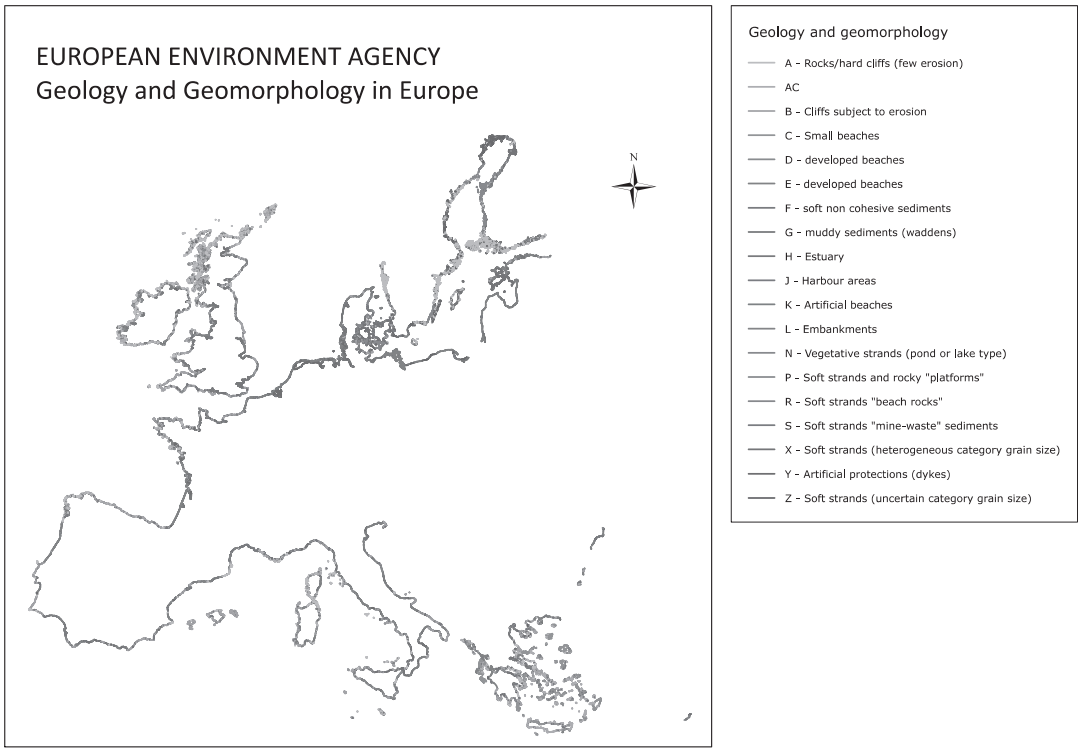

Figure 2. European geology and geomorphology (EEA, 2009).

individual parameters. Next, the composite vulnerability needs to be calculated and ranked for each individual cell using Equation (1).

All CVI applications to date classify (or rank) the composite vulnerability values obtained by applying Equation (1) into the 25th, 50th, and 75th percentiles. As a result, the classification procedure distinguishes between four possible classes: 0–25th percentile: low; 25th–50th percentile: medium; 50th–75th percentile: high; and 75th–100th percentile: very high. As such, a *very low* vulnerability class is absent in previous applications.

In this study, to be consistent with the classification of the six individual parameters into 5 separate categories, the composite vulnerability is also classified into 5 categories, thus enabling a *very low* vulnerability class. This is achieved by modifying the ranking ranges to 0–20th percentile (very low), 20th–40th percentile (low), 40th–60th percentile (medium), 60th–80th percentile (high), and 80th–100th percentile (very high).

Application of the CVI for the Spanish Coast

This section will describe how each component of the CVI has been quantified for the specific case of the Spanish coastline.

x_1: Geomorphology

The geomorphology along the Spanish coast, as obtained from the EEA (2009), is shown in Figure 2. The online database of the European Environment Agency (EEA, 2009) contains maps of geomorphology that can be interrogated with ArcGIS (1:100,000-scale map, last updated in 2009, in vector format and comprising a segmentation of the EUROSION shoreline. Geographical coverage note: Romania, Bulgaria, Cyprus, and ultraperipheral regions are only covered 20%. Also, only EU25 countries with coasts are included in the data set.)

After careful analysis of the information presented in the figure, the different landforms along the Spanish coast were classified into 5 vulnerability classes as shown in Table 2 (top row).

x_2: Shoreline Erosion/Accretion

The historical shoreline evolution data available from the EEA (2009), which provides the main trends at a broad spatial scale along European coasts (last updated in 2004, 1:100,000 resolution, only relates three different types of behaviour: accretion (aggradation), stable, and erosion. Therefore, unlike previous applications of the CVI (*e.g.,* Abuodha and Woodroffe, 2006), which considered five shoreline-evolution categories, here, the above three behavioral types were directly assigned very low, moderate, and very high vulnerability classes as shown in Table 2 (second row).

x_3: Coastal Slope

The mean slope, calculated as described in the section "Components of CVI," using the GEBCO (2014) bathymetry (for submerged slope) and Google Earth 7.0.2.8415beta (2015) (for subaerial slope, through images with 1:5000 resolution and dated at different times) was classified into five vulnerability classes: 0–0.02: very high; 0.02–0.04: high; 0.04–0.08: moderate; 0.08–0.12: low; and >0.12: very low (Table 2, row 3).

Table 2. *Summary of the classification criteria applied to each variable.*

Variable	Evaluated Features	Vulnerability Classification				
		1: Very Low	2: Low	3: Moderate	4: High	5: Very High
Geomorphology	Qualitative features	Rocks/ hard cliffs (little erosion)	Embankments	Cliffs subject to erosion	Soft shores ("beach rocks")	Small beaches
				Vegetative shores (pond or lake type)	Soft shores ("mine-waste" sediments)	Developed beaches
		Harbour areas	Artificial protections (dykes)	Soft shores and rocky "platforms"	Soft shores (heterogeneous category grain size)	Soft, noncohesive sediments
				Muddy sediments (waddens)	Estuary	Artificial beaches
						Soft shores (uncertain category grain size)
Shoreline erosion/ accretion	Erosion or acretion length[a]	Accretion (>+1 m/y)		Stable (−1 to +1 m/y)	—	Erosion (<−1 m/y)
Slope	Mean slope (%)	>12	8–12	4–8	2–4	<2
Relative SLR	Relative SLR (m, by 2100)	—	0–0.18	0.18–0.38	0.38–0.59	0.59–1
	Linked Scenario	—	Low emission	Medium emission	High emission	"Worst-case" emissions
Wave climate	$H^2_{s_{95\%}}/H^2_{s_{threshold}}$	<0.65	0.65–0.75	0.75–1	1–1.5	>1.5
Mean tide gauge	Tidal range (m)	>6.0	4.0–6.0	2.0–4.0	1.0–2.0	<1.0

[a] Note: Erosion rates are considered negative (<0), and accretion rates are shown as positive (>0)

Figure 3. Wave buoys (circles) and tide gauges (triangles) locations along the Spanish coast (Puertos del Estado, 2012).

x_4: Relative SLR

Historical water level statistics were obtained from the public service *Puertos del Estado*. These statistics are calculated using the data collected by the network of 20 tidal gauges (see Figure 3) maintained by the Ministry of Public Works along the entire Spanish coastline.

The potential range of global average eustatic SLR was directly taken as given in IPCC (2007) (Table 1). Apart from vertical land movement, all other contributors to RSLR, as indicated in Equation (2) can reasonably be neglected along the Spanish coastline. Land subsidence is reported at several locations along the Spanish coastline (Table 3) (Cendrero, Sánchez-Arcilla Conejo, and Zazo Cardeña, 2005; Copons, 2008). Although the subsidence in different areas is slightly different, for this national-scale assessment, an average subsidence rate of 2 mm/y appears to be an appropriate approximation for all areas affected by subsidence (Somoza *et al.*, 1998). Therefore, in all areas affected by subsidence, 2 mm/y was added to the IPCC-projected global average SLR values to obtain the RSLR estimates. Following the rationale described in the "Components of the CVI" section, the RSLR was classified into four vulnerability classes as shown in Table 2 (row 4).

x_5: Wave Climate

Wave statistics from the 35 buoys maintained by the Ministry of Public Works were used in this study. Most buoys have been recording data for more than 10 years. The data have already been analyzed, and wave statistics are available in two forms: a mean-wave climate report (Puertos del Estado, 2012), which provides statistics on all measured wave conditions, and an extreme-wave climate report (Puertos del Estado, 2012), which only provides statistics on the high-energy wave events (storms). The 95th percentile significant wave height ($H^2_{s_{95\%}}$) for each buoy was obtained from the former, whereas the latter was used to obtain a significant wave-height threshold ($H^2_{s_{threshold}}$) that defines storms using the POT (Peak over Threshold) approach. This threshold will define a storm at each location, and its value depends very much on the local conditions. The criterion is that a sufficient number of storms (preferably several dozen or more) can be identified in the long-term time record (to be considered a storm each individual storm event must occur at least 5 days before the next one). The

Table 3. *List of Spanish coastal zones affected by subsidence.*

Autonomous Region in Spain	Zone Affected by Subsidence
Catalonia	Empordà plain/Gulf of Roses
	Tordera Delta
	Besós Delta
	Llobregat Delta
	Ebro Delta
Valencian community	Marjal Oliva-Pego
	Albufera València
	Salines Santa Pola
	Dunas guardamar (Guardamar de Segura)
Murcia	Menor Sea
Andalucía	Doñana

Spanish regulation ROM 03.91 displays the threshold for each sector. Those two values were then used in Equation (4) (see the Methods section) for each buoy. The range of values thus obtained were subsequently classified into five vulnerability classes, as shown in Table 2 (row 5) following the rationale described in section 2.1.

x_6: Tidal Range

The tidal range varies substantially along the Spanish coastline, from 1.5 and 4 m along the Cantabrian and Galician coastline to about 3 m along the mostly mesotidal Atlantic Andalusian coast. The Mediterranean coastline is microtidal with tidal ranges less than 1 m (Cendrero, Sánchez-Arcilla Conejo, and Zazo Cardeña, 2005).

For the CVI application, the maximum tidal range, calculated at each of the 20 tide gauges around Spain, was used to obtain five vulnerability classes following the same rationale as adopted by Pendleton *et al.*, (2004) for the US coast and Ojeda Zújar *et al.*, (2009) for the Andalusian coast. The adopted vulnerability classes are shown in Table 2 (last row).

Selected Scale

To implement the aggregation methodology described in the "Aggregation procedure" section, the Spanish coastline was discretized into 135 individual cells to accommodate the spatial variation of geomorphology, historical shoreline evolution, coastal slope, RSLR (*via* variations in subsidence) wave climate, and tidal range. As mentioned in the Methods section, eustatic SLR was reasonably assumed to be a spatial invariant, and as such, only one value per emissions scenario was used in the CVI calculations. However, four different SLR values were considered corresponding to low, medium, high, and worst-case emission scenarios, resulting in four different national vulnerability maps (one per emission scenario).

The range of CVI values thus obtained (encompassing all four different emission scenarios; span 2.236 to 45.644, Table 4). To ensure that the vulnerability assessment accounted for the large uncertainty, particularly in the SLR projections, the 20th, 40th, 60th, and 80th percentiles of CVI values were calculated using all CVI estimates obtained for all emissions scenarios (instead of per scenario). The overall vulnerability-assessment scheme based on the CVI percentiles thus obtained is shown in Table 5. The four coastal vulnerability maps (resulting from the 4 RSLR scenarios) are shown in Figure 4.

Table 4. *Minimum and maximum values obtained for the different emission scenarios.*

Considered Scenario	Minimum Value	Maximum Value
Low-emission scenario	2.236	35.355
Medium-emission scenario	2.739	40.825
High-emission scenario	3.162	45.644
"Worst-case" emission scenario	3.536	45.644

RESULTS

Figure 4 clearly show that higher SLR will result in higher vulnerability all along the Spanish coastline. The variation in vulnerability with the RSLR scenario is further illustrated by Table 6, which tabulates the percentage of coastline (in kilometers) that falls into each vulnerability class per RSLR scenario.

Vulnerability Classification Along the Coast

With the low emission scenario, 24.6% of the coast is highly or very highly vulnerable. Under this scenario, there are four main vulnerable areas that are in close proximity to deltas: Ebro, Besos, Llobregat, and Guadalquivir, among others. Other areas that are highly or very highly vulnerable under this RSLR scenario are The Gulf of Cádiz and the regions of Málaga, Alicante, Tarragona, Valencia, and Murcia, whose main reasons for vulnerability are stated in Table 7. Table 8 presents the total CVI and the value of each individual parameter for these areas.

Under the medium RSLR scenario, not surprisingly, a larger extension of the Spanish coastline is vulnerable. The percentage of coastline that falls into the low and very low vulnerable classes decreases by more than 18%. The occurrence of high and very high vulnerability classes increases to 32%, an increase of approximately 10% compared with the low-emissions scenario. The additional highly vulnerable areas are mostly located next to those identified under a low-emissions scenario. Compared with the low-emission scenario, additional vulnerable areas are shown in the vicinity of the Ría de Arosa; some locations in Barcelona (el Maresme and Castelldefels/Garraf), Castelló, Almería, and Cádiz, where long open beaches comprising soft sands make them highly vulnerable; and in Almería also near river mouths. The main reasons for the vulnerability of these areas are shown in Tables 9 and 10.

Under the high-emissions scenario (SRL = 0.6 m), the high- and very high-vulnerability classes represent 38.6% of the entire coastline, a marginal increase of 6% from the medium-emissions scenario case. The spatial distribution of the coastal stretches with different vulnerability is generally the same as that for the medium-emissions scenario, but in a few cases the singular vulnerability of the stretches is enhanced. The additional vulnerable locations (compared with the medium-emissions scenario) are mostly around the vulnerable locations

Table 5. *Adopted overall vulnerability scheme.*

Vulnerability Class				
Very Low	Low	Moderate	High	Very High
2.236–6.928	6.928–10.206	10.206–13.693	13.693–20	20–45.644

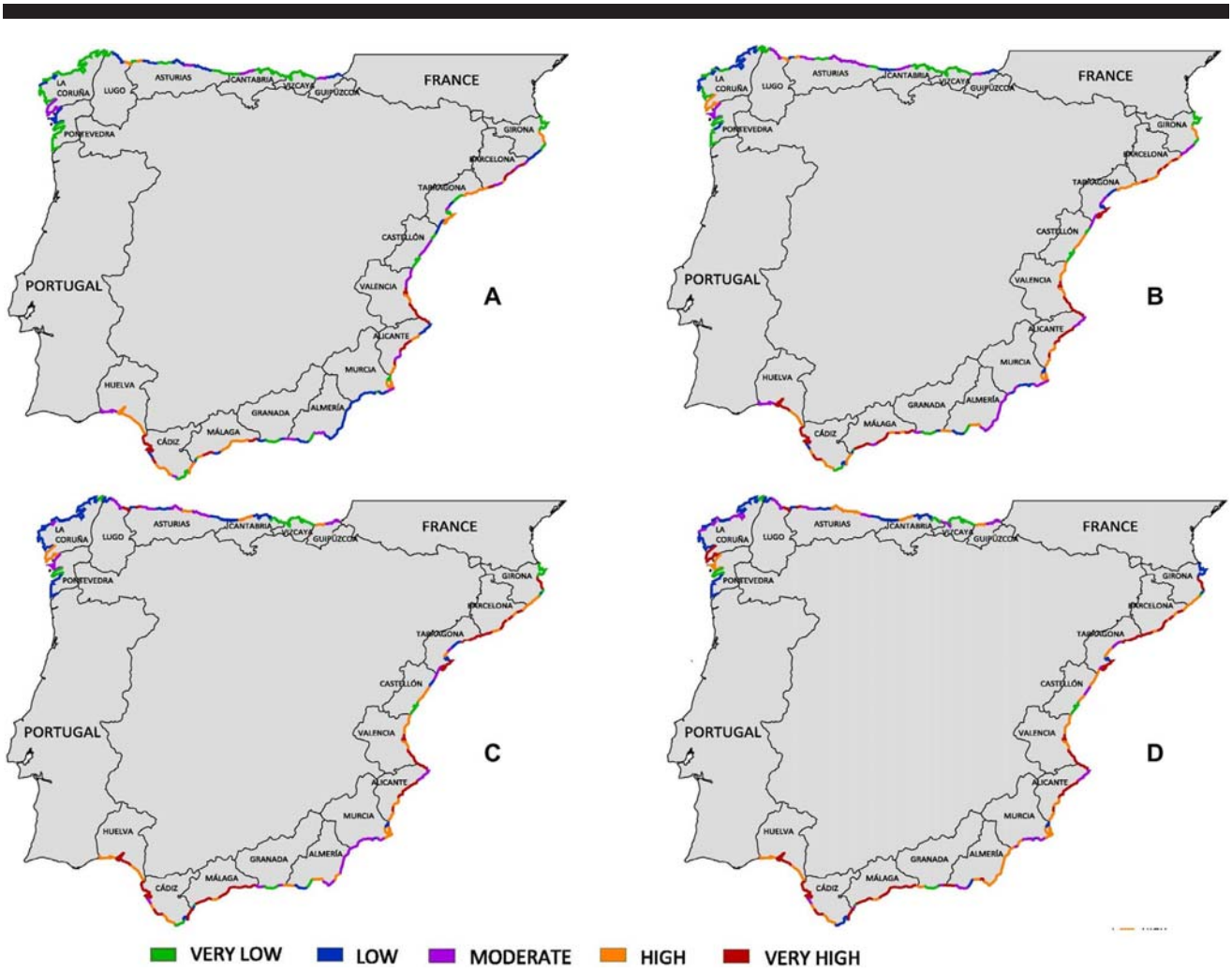

Figure 4. CVI distribution along the Spanish coast for analyzed scenarios. (A: low; B: medium; C: high; D: worst case). (Color for this figure is available in the online version of this paper.)

that were identified for the medium-emissions scenario, but the vulnerability is emphasized.

Finally, under the worst-case SLR scenario (SLR = 1 m), 50% of the Spanish coastline falls under the high- or very high-vulnerability classes. The main new, additional, highly vulnerable areas and their CVI values are listed in Tables 11 and 12, and the overall CVI for each individual stretch under this scenario is given in Table 13.

The above results compare rather well with the higher-resolution regional CVI application reported by Ojeda Zújar *et al*., (2009) for Andalucia. A direct comparison is, however, impossible because of the differences in resolution, differences in the way the individual parameters were calculated, and the differences in the assigned composite vulnerability classes (five classes in the present study *vs*. four in the study by Ojeda Zújar *et al*., 2009).

Because the Ojeda Zújar *et al*. (2009) study used historically observed SLR trends, whereas the present study used IPCC-projected SLR trends, for comparison purposes, we examine the results of our medium-emissions scenario, which is neither too optimistic nor pessimistic, with the results from the Ojeda Zújar *et al*. (2009) study. Furthermore, because of the aforementioned differences in the number of composite vulnerability classes (four *vs*. five), here, we compare our moderate- and high-vulnerability classes with the Ojeda Zújar *et al*. (2009) high-vulnerability class.

Table 6. *Percentage of coastline (in kilometers) that falls into each vulnerability class per RSLR scenario.*

	Emission Scenario			
Classification	Low	Medium	High	Worst Case
Very low	40.3	22.8	11.5	7.2
Low	23.4	22.5	30.0	26.1
Medium	11.7	23.2	19.9	17.1
High	18.0	16.0	19.9	26.8
Very high	6.6	15.4	18.7	22.9

Table 7. *Main vulnerable areas under the low-emission scenario.*

Region Name	Stretch No.[a]	Main Reasons for Vulnerability
Ebro Delta	24	Unfavorable geomorphology, subsidence, small tidal range, gentle slope
Besos Delta	12	Unfavorable geomorphology, subsidence, small tidal range, gentle slope
Llobregat Delta	14	Unfavorable geomorphology, subsidence, small tidal range, gentle slope
Tarragona	17	Unfavorable geomorphology, small tidal range, gentle slope, erosive coastline trend
Valencia	34–38	Unfavorable geomorphology, erosive shoreline trend, small tidal range, subsidence
Alicante	40–44	Erosive shoreline trend, small tidal range
Murcia (Menor Sea)	47, 48	Unfavorable geomorphology, gentle slope, subsidence
Málaga	70–80	Erosive shoreline trend, gentle coastal slope, small tidal range
Gulf of Cádiz	91	Unfavorable geomorphology, erosive shoreline trend, gentle slope

[a] See Figure 4.

Table 8. *Individual parameters for the mentioned vulnerable areas under the low-emission scenario.*

Parameter	Besos	Llobregat	Tarragona	Ebro	Valencia	Alicante	Murcia	Málaga	Gulf of Cádiz
Stretch number[a]	12	14	17	24	38	41	47, 48	79	91
Geomorphology	5	5	5	5	5	3	5	4	5
Shoreline erosion/accretion	5	1	5	5	5	5	3	5	5
Coastal slope	4	5	5	5	5	4	5	5	4
Sea-level rise	3	3	2	3	3	2	3	2	3
Wave height	4	4	4	1	4	4	1	3	3
Tide range	5	5	5	5	5	5	5	5	3
Total CVI	31.62	15.81	28.87	17.68	35.36	20.00	13.69	22.36	21.21
Vulnerability[b]	VH	H	VH	H	VH	VH	H	VH	VH

[a] See Figure 4.
[b] VH = very high, H = high.

Table 9. *Main vulnerable areas under the medium-emission scenario.*

Region Name	Stretch No.[a]	Main Reasons for Vulnerability
Barcelona (el Maresme)	7, 9	Erosive shoreline trend, gentle slope, small tidal range
Barcelona (Castelldefels/Garraf)	15, 16	Erosive shoreline trend, gentle slope, small tidal range
Castelló	29, 30	Soft sands (unfavorable geomorphology), gentle slope, small tidal range
Almería (Costacabana)	60, 61	Soft sands (unfavorable geomorphology), gentle slope, small tidal range
Almería (Delta Adra)	64	Unfavorable geomorphology, gentle slope, erosive coastline trend
Cádiz (Valdevaqueros)	86	Unfavorable geomorphology, erosive coastline trend, small tidal range
Ría de Arosa	100	Unfavorable geomorphology, energetic wave climate

[a] See Figure 4.

Table 10. *Individual parameters for the mentioned vulnerable areas under the medium-emission scenario.*

Parameter	Barcelona (Maresme)	Castelldefels/ Garraf	Castelló	Almería (Costacabana)	Almería (Delta Adra)	Cádiz (Valdevaqueros)	Ría de Arosa
Stretch number[a]	7, 9	15, 16	29, 30	60, 61	64	86	100
Geomorphology	1	1	5	5	4	5	5
Shoreline erosion/accretion	5	5	5	5	5	5	3
Coastal slope	4	5	3	4	5	3	4
Sea-level rise	3	3	3	3	3	4	3
Wave height	4	4	1	1	1	1	3
Tide range	5	5	5	5	5	4	3
Total CVI	14.14	15.81	13.69	15.81	15.81	14.14	16.43
Vulnerability[b]	H	H	H	H	H	H	H

[a] See Figure 4.
[b] H = high.

Both studies predict moderate vulnerability for the first tens of kilometers of the Huelva region and a rise in vulnerability to the highest class (*very high* at Punta Umbría, decreasing thereafter to *high*, and remaining so up to Cádiz).

Along the coastline of Cádiz, both studies show the Cabo de Gata is to be a very vulnerable area. Both studies also indicate a radical change from high to low vulnerability when approaching Tarifa (from the west), and that it remains low until Gibraltar. The Ojeda Zújar *et al.* (2009) study shows many changes in vulnerability within a short distance in Málaga, Granada, and Almería, which are not apparent in the present study because of its poorer resolution.

Martí López (2011) reports a detailed vulnerability assessment for Catalonia using methodologies that are rather different to that adopted in the present study. The final conclusion in the Martí López's (2011) study was that the coastline in Catalonia was highly vulnerable to erosion because of RSLR, and in the long term, because of longshore transport,

Table 11. *Main vulnerable areas under the "worst-case" emission scenario.*

Region Name	Stretch No.[a]	Main Reasons for Vulnerability
Barcelona (Lloret de Mar)	6	Erosive shoreline trends, small tidal range, sea-level rise
Tarragona (Hospitalet Infant)	21, 22	Erosive shoreline trends, small tidal range, sea-level rise
Castelló (Vinarós)	26, 27	Erosive shoreline trends, small tidal range, sea-level rise
Murcia (Cabo de Palos)	49	Gentle slope, sea-level rise, small tide range
Murcia	53	Gentle slope, sea-level rise, small tide range
Almería (Cabo de Gata)	55, 56, 57, 58, 59	Erosive shoreline trends, gentle slope, sea-level rise
Granada (Almuñecar)	69	Erosive shoreline trends, sea-level rise, small tide range
Málaga (Calahonda)	75	Erosive shoreline trends, sea-level rise, small tide range
Pontevedra (Ría de Pontevedra)	99	Unfavorable geomorphology, gentle slope, sea-level rise
Asturias (Gijón)	120, 121, 122, 123	Erosive shoreline trend, sea-level rise
Cantabra (Ría de Suances)	127	Erosive shoreline trend, gentle slope, sea-level rise
Gipuzkoa (Río Urola)	134	Erosive shoreline trend, gentle slope, sea-level rise

[a] See Figure 4.

has a low vulnerability to inundation because of RSLR (although some deltaic areas portray high vulnerability), and low vulnerability to erosion because of storm impacts. In general terms, Martí López (2011) concluded that the average vulnerability of the Catalan coastline was high.

To reasonably compare the outcomes of both studies, they need to be based on the same assumptions, and therefore, we compare our results with those of the approach that follows the same method as the CVI assessment for the U.S. Pacific Coast used by Martí López (2011) for the third SLR scenario (0.59 m of SLR in 100 y).

Both approaches indicate that the northmost Catalonian province of Girona is of low vulnerability, mainly because of the presence of coarse sediments on the beaches. Moving south, both approaches indicate the Aiguamolls de l'Empordà (Marshes of Empordà) is a very vulnerable formation.

The Martí López (2011) Catalan vulnerability index offers more resolution and thus more spatial variability along the coastline, pointing out some small areas with low vulnerability surrounded by more extensive and highly vulnerable areas, which cannot be identified by the coarser resolution at the national-scale with the CVI application in the present study. This is the case in the southern coastline of the province of Girona, which is shown to be highly vulnerable in its entirety in the present study, whereas the higher resolution in the Martí López (2011) study shows stretches with both moderate and high vulnerability in this region.

The Barcelona region is shown to have a combination of both high and very high vulnerability by both approaches, peaking in a high vulnerability around the Llobregat delta. However, the Martí López (2011) approach detects some short stretches with individual features, and thus with a specific vulnerability (different to the surroundings), which cannot be detected by the coarse-scale of the CVI application in the present study.

Both approaches also show the spatial variability in vulnerability in the province of Tarragona consistently, indicating the increase in vulnerability round the Ebro delta, a highly vulnerable delta suffering from a serious combination of subsidence and a lack of sediment supply.

DISCUSSION

A more detailed description of the distribution of coastal vulnerability along the Spanish coast is given below.

Very Vulnerable Zones

The vulnerability assessment highlights some areas as being very vulnerable even under the most optimistic emissions scenario. Most of these areas are located along the Mediterranean coast containing the longest uninterrupted soft-sand beaches of the Spanish coastline (Table 7).

Many examples are found along the Catalan coast, especially along the southern part, as well as along Málaga, Valencia, and Alicante, the latter two having some of the most unfavorable combination of geomorphology and erosion trends.

Some deltas along the Mediterranean coast are also classified as highly vulnerable, the most important of which is the Ebro delta, where both subsidence and the scarcity of sediments make it very vulnerable. Further to the south, the subsiding coastal formation in the Menor Sea, in the province of Murcia, also appears to be vulnerable in most of the considered emissions scenarios.

The coastline of the gulf of Cádiz, located on the Atlantic coast of Andalucía, is another highly vulnerable area. The high vulnerability of this area, which contains the Doñana National Park with its fragile dune systems that give shape to an important wetland and the Guadalquivir's mouth, is mostly due to the presence of low cliffs with a high potential of retreat, long sand barriers, and river mouths.

Moderately Vulnerable Zones

The coasts in Barcelona and the surrounds of the Catalan deltas are shown to be moderately vulnerable as RSLR increases. Some areas in Almería and Valencia also fall within the moderately vulnerable category, particularly where there are open, sandy beaches or seasonal rivers that transport significant volumes of sand into deltas in the Mediterranean (*e.g.*, delta of Adra) during flood events.

Along the northern Cantabrian and Atlantic coast, some rías appear to be of moderate vulnerability. These river mouths or estuaries shelter wetlands, marshes, and small beaches and, therefore, represent potentially fragile areas under the less-optimistic emissions scenarios. Some examples are Ría de Arosa, the Ría de Vigo, and the Ría de Ribadeo.

Less-Vulnerable Zones

Essentially, all parts of the Spanish coastline that have not been mentioned in the previous two categories can be considered to be less vulnerable.

Table 12. *Individual parameters for the mentioned vulnerable areas under the "worst-case" emission scenario.*

Parameter	Barcelona (Lloret de Mar)	Tarragona (Hospitalet Infant)	Castelló (Vinaròs)	Murcia (Cabo de Palos)	Murcia (certain spots)	Almería (Cabo de Gata)	Granada (Almuñecar)	Málaga (Calahonda)	Pontevedra (Ría de Pontevedra)	Asturias (Gijón)	Cantabra (Ría de Suances)	Gipuzkoa (Río Urola)
Stretch No.[a]	6	21, 22	26, 27	49	53	55–59	69	75	99	120–123	127	134
Geomorphology	1	3	3	3	3	3	3	4	5	3	3	3
Shoreline erosion/accretion	5	5	5	3	3	5	5	5	1	5	5	5
Coastal slope	3	3	3	5	5	4	3	1	5	3	4	4
Sea-level rise	5	5	5	5	5	5	5	5	5	5	5	5
Wave height	4	1	1	1	1	1	1	3	3	3	3	3
Tide range	5	5	5	5	5	5	5	5	3	2	2	2
Total CVI	15.81	13.69	13.69	13.69	13.69	15.81	13.69	15.81	13.69	15.00	17.32	17.32
Vulnerability[b]	H	H	H	H	H	H	H	H	H	H	H	H

[a] See Figure 4.
[b] H = high.

The Cantabrian coastline is obviously the least-vulnerable stretch of coastline in Spain. Mountain chains, which often reach into the sea, are common in this area, implying a favorable geomorphology averting vulnerability. The larger tidal ranges experienced in this area also contribute to the lower vulnerability of the region.

Along the Mediterranean coast, there are some isolated locations that appear to be of low vulnerability, even under the high-emissions scenarios. For instance, along the northern tip of Girona's coastline, the coast is mostly rocky and comprises cliffs combined with pocket beaches made of coarse sands, a combination of factors that will certainly make this part quite resilient. The SE corner of Cádiz, where the Atlantic Ocean meets the Mediterranean Sea, is another such area that shows a low vulnerability because, although the geomorphology of this vulnerable area is not much different from the surrounding areas of Cádiz, the wave energy here is less than elsewhere in this mostly vulnerable province.

Although the approach described and demonstrated above provides a very useful "first-pass" assessment of coastal vulnerability at a national scale, the results do incorporate a high level of uncertainty because of the use of relatively low-resolution spatiotemporal information (*e.g.,* shoreline movements from infrequent aerial photographs, deepwater wave heights, geomorphic classification, global averaged SLR, *etc.*). Therefore, it would be prudent to undertake more-detailed, local-scale assessments for areas identified by the above approach as being more vulnerable than the average, especially if the potential risk to communities/developments is also high in such areas.

CONCLUSIONS

One of the major obstacles in undertaking national-scale, coastal-vulnerability assessments, particularly when faced with limited budgets, is the nonavailability of an assessment method that requires only easily accessible data and is easy to use. This study has developed a method that satisfies both of those requirements.

The method developed herein is a modified version of the Coastal Vulnerability Index (CVI) approach. The main modifications are (1) the introduction of a representation of the wave effect that is more meaningful physically because storm erosion only occurring when the wave height exceeds a certain threshold value is accounted for, and (2) an aggregated coastal-vulnerability classification method that comprises exactly the same number of vulnerability classes as that of the individual components of the CVI.

The method was applied to the 4996-km-long, peninsular coastline of Spain as a demonstration application. Results indicate that even under the most-optimistic greenhouse gas emissions scenario, some parts of the Mediterranean coast will have high or very high vulnerability. Results indicate that under the worst-case emissions scenario considered (SLR of 1 m by 2100), 50% of the Spanish coastline is highly or very highly vulnerable, whereas 33% of the coastline indicates low or very low vulnerability. Even under the most-optimistic greenhouse gas emissions scenario, some parts of the Mediterranean coast will have high or very high vulnerability. Given that 10% of the Spanish GDP is generated *via* tourism, it is

Table 13. *Overall CVI classification under the "worst-case" scenario.*

Stretch No.[a]	CVI	Vunerability[b]
1	7.071	L
2	20.412	VH
3	7.071	L
4	7.906	L
5	6.455	VL
6	15.811	H
7	18.257	H
8	40.825	VH
9	18.257	H
10	40.825	VH
11	18.257	H
12	40.825	VH
13	35.355	VH
14	20.412	VH
15	20.412	VH
16	18.257	H
17	45.644	VH
18	22.822	VH
19	22.822	VH
20	10.206	M
21	13.693	H
22	13.693	H
23	7.906	L
24	22.822	VH
25	12.910	M
26	13.693	M
27	13.693	M
28	7.906	M
29	17.678	H
30	17.678	H
31	5.000	VL
32	6.455	VL
33	18.257	H
34	45.644	VH
35	18.257	H
36	45.644	VH
37	35.355	VH
38	45.644	VH
39	12.247	M
40	27.386	VH
41	31.623	VH
42	17.321	H
43	27.386	VH
44	18.257	H
45	17.678	H
46	7.906	L
47	17.678	H
48	17.678	H
49	13.693	H
50	12.247	M
51	8.660	L
52	10.607	M
53	13.693	H
54	12.247	M
55	13.693	H
56	14.434	H
57	14.142	H
58	15.811	H
59	13.693	H
60	20.412	VH
61	18.257	H
62	7.071	L
63	10.206	M
64	20.412	VH
65	12.910	M
66	3.536	VL
67	3.536	VL
68	4.564	VL
69	13.693	H
70	31.623	VH
71	22.361	VH
72	27.386	VH
73	25.000	VH
74	30.619	VH
75	15.811	H
76	31.623	VH
77	31.623	VH
78	31.623	VH
79	35.355	VH
80	30.619	VH
81	6.124	VL
82	11.180	M
83	22.361	VH
84	10.000	L
85	7.071	L
86	15.811	H
87	17.678	H
88	23.717	VH
89	19.365	H
90	10.607	M
91	27.386	VH
92	8.660	H
93	23.717	VH
94	13.693	H
95	8.216	L
96	8.216	L
97	9.487	L
98	6.124	VL
99	13.693	H
100	21.213	VH
101	8.216	L
102	9.487	L
103	10.954	M
104	7.746	L
105	12.247	M
106	8.660	L
107	10.607	M
108	8.660	L
109	10.607	M
110	8.944	L
111	8.944	L
112	6.325	VL
113	7.746	L
114	13.416	M
115	22.361	VH
116	10.000	L
117	22.361	VH
118	13.416	M
119	7.746	L
120	15.000	H
121	15.000	H
122	17.321	H
123	15.000	H
124	13.416	M
125	7.746	L
126	9.487	L
127	17.321	H
128	7.746	L
129	7.746	L
130	6.708	VL
131	13.416	M
132	6.708	VL
133	6.708	VL
134	17.321	H
135	12.247	M

Table 13. *Continued.*

[a] See Figure 4.
[b] L = low, VH = very high, VL = very low, H = high, M = medium.

noteworthy that these vulnerable zones are also among the most touristic locations along the Spanish coast, containing beaches, deltas, estuaries, and lagoons.

The relative simplicity of the coastal-vulnerability assessment method presented here makes it easy to use (even by nonexperts) and easily adaptable to other parts of the world. The outcome of national-scale, first-pass vulnerability assessments undertaken using this method will enable coastal managers/planners to identify high-priority areas for further, more-detailed coastal vulnerability/hazard/risk quantification studies. In this sense, this simple approach can significantly contribute to the implementation of planning strategies along the Spanish coastal zone and elsewhere. As an example, these results provide a quick avenue to satisfy the recommendations of the Protocol on Integrated Coastal Zone Management in the Mediterranean to undertake vulnerability and hazard assessments regarding natural disasters and, in particular, to determine CC impacts. In addition, these results can be used to identify highly vulnerable areas to define priority-action zones along the coast in which to implement measures considered within the Spanish National Climate Change Adaptation Plan.

ACKNOWLEDGMENTS

Roshanka Ranasinghe is supported by the AXA Research fund and the Deltares Harbour, Coastal and Offshore Engineering Research Programme *Bouwen aan de Kust*. The work of the third author was done in the framework of the RISES-AM (Grant No. 603396) and PaiRisC-M (CTM2011-29808) research projects funded by the EU and the Spanish Ministry of Economy and Competitiveness, respectively.

LITERATURE CITED

Abuodha, P.A. and Woodroffe, C.D., 2006. Assessing vulnerability of coasts to climate change: A review of approaches and their application to the Australian coast. *In:* Woodroffe, C.D.; Bruce, E.; Puotinen, M., and Furness. R.A. (eds.), *GIS for the Coastal Zone: A Selection of Papers from CoastGIS 2006*. Wollongong, Australia: Australian National Centre for Ocean Resources and Security, University of Wollongong, 458p.

Abuodha, P.A.O., 2009. Application and Evaluation of Shoreline Segmentation Mapping Approaches to Assessing Response to Climate Change on the Illawarra Coast, South East Australia. Wollongong, Australia: School of Earth and Environmental Sciences, University of Wollongong, Ph.D. dissertation, 286p.

Bosom, E. and Jiménez, J.A., 2011. Probabilistic coastal vulnerability assessment to storms at regional scale- application to Catalan beaches (NW Mediterranean). *Natural Hazards and Earth System Sciences,* 11, 475–484.

Brown, S.; Nicholls, R.J.; Hanson, S.; Brundrit, G.; Dearing, J.A.; Dickson, M.E.; Gallop, S.L.; Gao, S.; Haigh, I.D.; Hinkel, J.; Jiménez, J.A.; Klein, R.J.T.; Kron, W.; Lázár, A.N.; Freitas Neves C.; Newton, A.; Pattiaratachi, C.; Payo, A.; Pye, K.; Sánchez-Arcilla Conejo, A.; Siddall, M.; Shareef, A.; Tompkins, E.L.; Vafeidis, A.T.; van Maanen, B.; Ward, P.J., and Woodroffe, C.D., 2014. Shifting perspectives on coastal impacts and adaptation. *Nature Climate Change,* 4, 752–755.

Bruun, P., 1962. Sea level rise as a cause of shore erosion. *Journal of the Waterways and Harbors Division,* 88, 117–130.

Cendrero Uceda, A.; Sánchez-Arcilla Conejo, A., and Zazo Cardeña, C., 2005. Impactos sobre las zonas costeras. *In: Evaluación Preliminar de los Impactos en España por Efecto del Cambio Climático*. Castilla la Mancha, Spain: Ministry of Environment, Universidad de Castilla-La Mancha, Proyecto ECCE–Informe final, pp. 469–524.

CLIMsystems, 2007. http://www.climsystems.com/about/about.php.

Copons, R., 2008. *El Risc d'Esfondraments i Subsidències a Catalunya*. Barcelona, Spain: Universitat de Barcelona, Consell Assessor per al Desenvolupament Sostenible, RISKCAT, pp. 1–29.

Domínguez, L.; Anfuso, G., and Gracia, F.J., 2005. Vulnerability assessment of a retreating coast in SW Spain. *Environmental Geology,* 47(8), 1037–1044.

EEA, 2009. http://www.eea.europa.eu/data-and-maps/figures/geology-and-geomorphology.

Gatriot, N.; Anthony, E.J.; Gardel. A.; Gaucherel, C.; Proisy, C., and Wells, J.T., 2008. Significant contribution of the 18.6 year tidal cycle to regional coastal changes. *Nature Geoscience,* 1, 169–172.

GEBCO (General Bathymetric Chart of the Oceans), 2014. http://www.gebco.net/.

Google Earth, 2015. http://www.google.es/intl/es/earth/index.html.

Gornitz, V. and Kanciruk, P., 1989. Assessment of global coastal hazards from sea level rise. *In:* Magoon, O.T. (ed.), *Coastal Zone '89, Proceedings of the 6th Symposium on Coastal and Ocean Management* (Charleston, South Carolina, ASCE), pp. 1345–1359.

Grabemann, I. and Weisse, R., 2008. Climate change impact on extreme wave conditions in the North Sea: An ensemble study. *Ocean Dynamics*, 58, 199–212.

Hemer, M.; Fan, M.; Mori, N.; Semedo, A., and Wang, X.L., 2013. Projected changes in wave climate from a multi-model ensemble. *Nature Climate Change,* 3, 471–476. doi:10.1038/nclimate1791

Hinkel, J. and Klein, R.J.T., 2009. Integrating knowledge to assess coastal vulnerability to sea-level rise: The development of the DIVA tool. *Global Environmental Change,* 19(3), 384–395.

Hinkel, J.; Nicholls, R.J.; Tol, R.S.J.; Wang, Z.B.; Hamilton, J.M.; Boot, G.; Vafeidis, A.T.; McFadden, L.; Ganopolski, A., and Klein, R.J.T., 2013. A global analysis of erosion of sandy beaches and sea-level rise: An application of DIVA. *Global and Planetary change,* 111, 150–158. doi:10.1016/j.gloplacha.2013.09.002

IPCC (Intergovernmental Panel on Climate Change), 2007: *Climate Change 2007: Synthesis Report. Contribution of Working Groups I, II, and III to the Fourth Assessment Report of the Intergovernmental Panel on Climate Change* [Core Writing Team, Pachauri, R.K and Reisinger, A. (eds.)]. Geneva, Switzerland: IPCC, pp. 104.

IPCC CZMS (IPCC Coastal Zone Management Subgroup), 1992. *Global Climate Change and the Rising Challenge of the Sea. Report of the Coastal Zone Management Subgroup, Intergovernmental Panel on Climate Change (IPCC) Working group III*. Rijkswaterstaat, The Netherlands: IPCC CZMS, 35pp + 5 appendices.

Kokot, R.R.; Codignotto, J.O., and Elissondo, M., 2004. Vulnerabilidad al ascenso del nivel del mar en la costa de la provincia de Río Negro. *Revista de la Asociación Geológica Argentina,* 59(3): 477–487.

Komar, P.D., 1998. *Beach Processes and Sedimentation,* 2nd edition. Upper Saddle River, New Jersey: Prentice Hall, 540p.

Málvarez García, G.; Pollard, J., and Domínguez Rodríguez, R, 2000. Origins, management, and measurement of stress on the coast of southern Spain. *Coastal Management,* 28, 215–234.

Martí López, M., 2011. Vulnerabilidad Física de la Costa Catalana a Diferentes Agentes. Barcelona, Spain: Departament d'Enginyeria Hidràulica, Marítima i Ambiental, Universitat Politècnica de Catalunya, Master's thesis, 178p.

Mendoza, E.T. and Jiménez, J.A., 2006. Storm-induced beach erosion potential on the Catalonian Coast. *In:* Alonso, I. and Cooper, J.A.G. (eds.), *Coastal Geomorphology in Spain: Proceedings of the Spanish Conference on Coastal Geomorphology*. Journal of Coastal Research, Special Issue No. 48, pp. 81–88.

Ministerio de Agricultura, Alimentación y Medio Ambiente, 2002. *Gestión integrada de las Zonas Costeras de España*. Madrid, Spain: Informe de España en cumplimiento de los requerimientos del capítulo VI de la Recomendación del Parlamento Europeo y del Consejo de 30 de Mayo de 2002 sobre la aplicación de la gestión integrada de las zonas costeras en Europa, 125 p.

Nicholls, R.J.; Hanson, S.; Lowe, J.A.; Warrick, R.A.; Lu, X., and Long, A.J., 2014. Sea-level scenarios for evaluating coastal impacts. *Wiley Interdisciplinary Reviews: Climate Change,* 5(1), 129–150.

Nicholls, R.J.; Wong, P.P.; Burkett, V.R.; Codignotto, J.O.; Hay, J.E.; McLean, R.F.; Ragoonaden, S., and Woodroffe, C.D., 2007. *Coastal Systems and Low-Lying Areas. Climate Change 2007: Impacts, Adaptation and Vulnerability. Contribution of Working Group II to the Fourth Assessment Report of the Intergovernmental Panel on Climate Change*, M.L. Parry, O.F. Canziani, J.P. Palutikof, P.J. van der Linden and C.E. Hanson, (eds.). Cambridge, U.K.: Cambridge University Press, 315–356.

NOAA (National Oceanic and Atmospheric Administration), 1999. Coastal Services Centre. http://www.csc.noaa.gov/.

Ojeda Zújar, J. J.; Álvarez Francoso, J.I.; Marín Cajaville, D., and Fraile Jurado, P., 2009. El uso de las TIG para el cálculo del índice de vulnerabilidad costera (CVI) ante una potencial subida del nivel del mar en la costa andaluza (España). *Revista Internacional de Ciencia y Tecnología de la Información Geográfica,* 9, 83–100.

Pendleton, E.A.; Williams S.J., and Thieler E.R., 2004. Coastal Vulnerability Assessment of Assateague Island National Seashore (ASIS) to Sea-level Rise. *U.S. Geological Survey Open-File Report 2004-1020*.

Pendleton, E.A.; Hammar-Klose, E.S.; Thieler, E.R., and Jeffress, W.S., 2004. Coastal Vulnerability Assessment of Gulf Islands National Seashore (GUIS) to Sea-Level Rise. *U.S. Geological Survey Open-File Report 03-108*.

Puertos del Estado, 2012. http://www.puertos.es/.

Ranasinghe, R. and Stive, M.J.F., 2009. Rising seas and retreating coastlines. *Climatic Change,* 97, 465–468. doi:10.1007/s10584-009-9593-3

Ranasinghe, R.; Callaghan, D., and Stive, M., 2012. Estimating coastal recession due to sea level rise: Beyond the Bruun Rule. *Climatic Change,* 110(3–4), 561–574.

Ranasinghe, R.; Duong, T.; Uhlenbrook, S.; Roelvink, D., and M. Stive, 2013. Climate change impact assessment for inlet-interrupted coastlines. *Nature Climate Change,* 3, 83–87. doi:10.1038/nclimate1664

Rosen, P.S., 1977. Increasing shoreline erosion rates with decreasing tidal range in the Virginia Chesapeake Bay. *Chesapeake Science,* 18(4), 383–386.

Sharples, J.; Moore, C.M.; Hickman, A.E.; Holligan, P.M.; Tweddle, J.F.; Palmer, M.R., and Simpson, J.H., 2009. Internal tidal mixing as a control on continental margin ecosystems. *Geophysical Research Letters,* 36, 23. doi:10.1029/2009GL040683

Slott, J.M.; Murray, A.B.; Ashton, A.D., and Crowley, T.J., 2006. Coastline responses to changing storm patterns. *Geophysical Research Letters,* 33. doi:10.1029/2006GL027445

Somoza, L.; Barnolas, A.; Arasa, A.; Maestro, A.; Rees, J.G., and Hernandez, F.J., 1998. Architectural stacking patterns of the Ebro delta controlled by Holence high-frequency eustatic fluctuations, delta-lobe switching and subsidence processes. *Sedimentary Geology,* 117, 11–32. doi:10.1016/S0037-0738(97)00121-8

SURVAS (Synthesis and Upscaling of Sea-level Rise Vulnerability Assessment Studies), 2004. UNFCCC, United Nations Framework Convention on Climate Change. http://unfccc.int/adaptation/nairobi_work_programme/knowledge_resources_and_publications/items/5490.php.

Thieler, E.R. and Hammar-Klose, E.S., 2000a. National Assessment of Coastal Vulnerability to Sea-Level Rise: Preliminary Results for the U.S. Pacific Coast. *U.S. Geological Survey Open-File Report 00-178*.

Thieler, E.R. and Hammar-Klose, E.S., 2000b. National Assessment of Coastal Vulnerability to Sea-Level Rise: Preliminary Results for the U.S. Gulf of Mexico Coast. *U.S. Geological Survey Open-File Report 00-179*.

United States Geological Survey (USGS), 2004. http://pubs.usgs.gov/of/2004/1020/html/rank.htm#table1.

UNFCCC (United Nations Framework Convention on Climate Change), 2008. http://unfccc.int/2860.php.

Vafeidis, A.T; Nicholls, R.J.; McFadden, L.; Tol, R.S.J.; Hinkel, J.; Spencer, T.; Grashoff, P.S.; Boot, G., and Klein, R.J.T., 2008. A new global coastal database for impact and vulnerability analysis to sea-level rise. *Journal of Coastal Research,* 24(4), 917–924.